Geophysical Research Letters

Supporting Information for

Antarctic pack-ice algal distribution: floe-scale spatial variability and predictability from physical parameters

K. M. Meiners[1,2,*,**] & S. Arndt[3,**], S. Bestley[4], T. Krumpen[3], R. Ricker[3,5], M. Milnes[1], K. Newbery[1], U. Freier[6], S. Jarman[1,7], R. King[1], R. Proud[8], S. Kawaguchi[1,2], B. Meyer[9,10,11]

1) Australian Antarctic Division, Department of the Environment and Energy, 203 Channel Highway, Kingston 7050, Tasmania, Australia

2) Antarctic Climate and Ecosystems Cooperative Research Centre, University of Tasmania, 20 Castray Esplanade, Hobart 7000, Tasmania, Australia

3) Alfred Wegener Institute, Helmholtz Centre for Polar and Marine Research, Sea Ice Physics, Bussestraße 24/27, 27570 Bremerhaven, Germany

4) Institute for Marine and Antarctic Studies, University of Tasmania, 20 Castray Esplanade, Hobart 7000, Tasmania, Australia

5) University of Brest, CNRS, IRD, Ifremer, Laboratoire d'Océanographie Physique et Spatiale (LOPS), IUEM, 29280, Brest, France

6) SC-Scientific Consulting, Münchener Str. 41a, 41472 Neuss, Germany

7) CIBIO-InBIO, Centro de Investigação em Biodiversidade e Recursos Genéticos, Universidade do Porto, R. Padre Armando Quintas nº 7, Vairão 4485-661, Portugal

8) Pelagic Ecology Research Group, Scottish Oceans Institute, Gatty Marine Laboratory, University of St Andrews, Fife KY16 8LB, Scotland, UK

9) Alfred Wegener Institute Helmholtz Centre for Polar- and Marine Research, section Polar Biological Oceanography, Am Handelshafen 12, 27570 Bremerhaven, Germany

10) Institute for Chemistry and Biology of the Marine Environment (ICBM), Carl von Ossietzky University Oldenburg, 26111 Oldenburg, Germany

11) Helmholtz Institute for Functional Marine Biodiversity Oldenburg (HIFMB), Germany, www.hifmb.de

*) Contact email: klaus.meiners@aad.gov.au

**) K. M. M. and S. A. contributed equally to this work

Contents of this file

Description of methods used for ice-core sampling, optical point-measurements and chlorophyll-a analysis:

Paired under-ice irradiance measurements and ice core samples were collected from 5 sites on the ice floe under investigation. These bio-optical sampling sites were chosen such that their immediate surroundings (5 m) showed no snow-cover disturbances, were level, and free of major surface deformations. On each sampling site we deployed a TriOS Ramses ACC VIS radiometer (Advanced Cosine Collector, 180° field of view) 0.15 m beneath the subsurface of the ice floe through an access hole (0.11 m diameter) using a retractable L-shaped stainless steel arm. The effect of the hole on the light measurements was assumed to be negligible due the position of the radiometer 1.2 m north (i.e., directed towards the sun) of the access hole. Under-ice high-resolution (400 - 700 nm, 3.3 nm band width) irradiance spectra were recorded with a laptop computer using TriOS MSDA_XE software version 7.5.1. Results used for further analyses represent average spectra calculated from of a minimum of 10 replicate radiometer measurements. At each site one ice core was collected directly above the radiometer location using a manual Kovacs Mark II ice core system (0.09 m core diameter). The sampled ice core was cut into 4 sections which were placed in clean polyethylene containers and transported back to the ship's laboratories. On the ship, sampled ice core sections were melted at 4°C in the dark within 24 – 36 hours of collection. After the ice cores had melted, the samples were gently mixed and samples taken for the determination of ice algal pigment concentration. For pigment analysis, 0.2 to 4.0 litres of melted ice core subsamples were filtered onto Whatman GF/F glass fibre filters, extracted with 90% (v/v) acetone and analysed for chl-a with a Turner Designs 10AU fluorometer according to standard protocols (*Melbourne-Thomas et al.*, 2015). Ice core section data (chl-a in μg l^{-1}) were integrated over the entire ice thickness and are expressed as integrated chl-a values (mg m^{-2}).

Calculation of Normalized Difference Indices:

The calculation of the Normalized Difference Index (NDI) to integrated ice core chl-a relationship exactly followed Melbourne-Thomas et al. (2015) and considered their corrigendum to the equations (*Melbourne-Thomas et al.*, 2016). Measured under-ice transmitted irradiance spectra were interpolated to consecutive integer (1 nm) wavelengths in the range of 400 to 700 nm, and normalised to the integrated under-ice irradiance over the 400 to 700 nm wavelength range in order to minimise the amplitude component of spectral variability and to focus on differences in spectral shape. The Normalized Difference Index for the wavelength pair 479 nm and 468 nm was then calculated as:

$$NDI\ (479{:}468) = [E_d(479nm) - E_d(468nm)] / [E_d(479nm) + E_d(468nm)] \quad (1)$$

In which E_d is the normalized intensity of under-ice irradiance in the specific wavelength bands (*Mundy et al.*, 2007; *Melbourne-Thomas et al.*, 2015, 2016*; Lange et al.*, 2016). NDI (479:468) values were related to log-normalized integrated chl-a values (SI, Fig. S1).

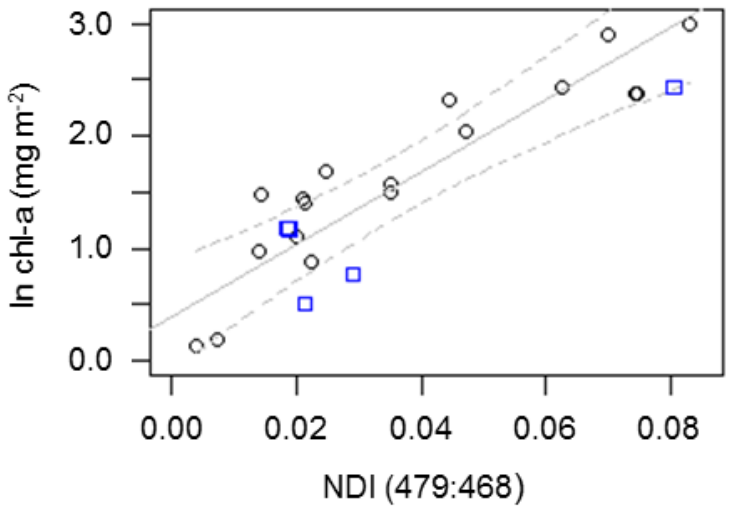

Figure S1: Normalized Difference Index (NDI) to integrated chlorophyll *a* concentration relationships. Black circles, regression line and 99% confidence intervals show the established relationship of Melbourne-Thomas et al. 2015 [$\ln (Chla_{ROV}) = 0.39 + 31.7 \times NDI_{(479:468)}$, $R^2 = 0.79$, $p < 0.0001$). Blue squares indicate measurements taken during this study (n = 5). For details see text.

Calculation of sea-ice freeboard levels:

Sea-ice freeboard levels (F) were calculated according to Arndt et al. (2017), as:

$$F = (I \times (\rho_w - \rho_i) - S \times \rho_s) / \rho_w \quad (2)$$

for positive freeboard.

Negative freeboard levels (-F), e.g., the flooded snow layer thickness were calculated as:

$$-F = S - ((I + S)/(1 + (\rho_s / (\rho_w - \rho_i)))). \quad (3)$$

The latter equation accounts for a change in density of snow once flooded. In these equations, S, I, ρ_s, ρ_w and ρ_i denote snow depth (m), ice thickness (m), density of snow (= 300 kg m^{-3}), density of water (= 1023.9 kg m^{-3}) and density of ice (= 915.1 kg m^{-3}), respectively.

Details on the instrumentation of the Remotely Operated Vehicle (ROV) used for under-ice surveys

Under-ice surveys were carried out using a SAAB SeaEye Falcon ROV instrumented with an upward-looking TriOS Ramses-VIS hyperspectral radiometer (320-950 nm) and an upward-looking Valeport500 sonar to measure under-ice irradiance and the distance between the sensor and the bottom of the ice, respectively. ROV position was determined using a long baseline (LBL) acoustic positioning system consisting of a Woods Hole Oceanographic Institution (WHOI) FSK micro-modem equipped with an ITC 3013 transducer (mounted to the ROV) and interrogating four Benthos XT-6001 transponders (15 m depth).

Statistical model results including spatial interaction

Figure S2 shows output from the GAM_{xy} model that includes a spatial smooth term (full tensor product interaction) on the x and y coordinates, in addition to the smooth functions for snow depth, ice thickness and ice freeboard. Note that the smooth functions for the biophysical terms remain almost identical to those shown in Fig. 4 (main text), with slightly widened confidence intervals but no substantive changes to the significance of terms. This indicates that even accounting for the strong spatial autocorrelation in the

dataset (GAM_{xy}: te(x,y), $p < 0.0001$, Fig. S2d) the algal relationships with biophysical drivers are strong.

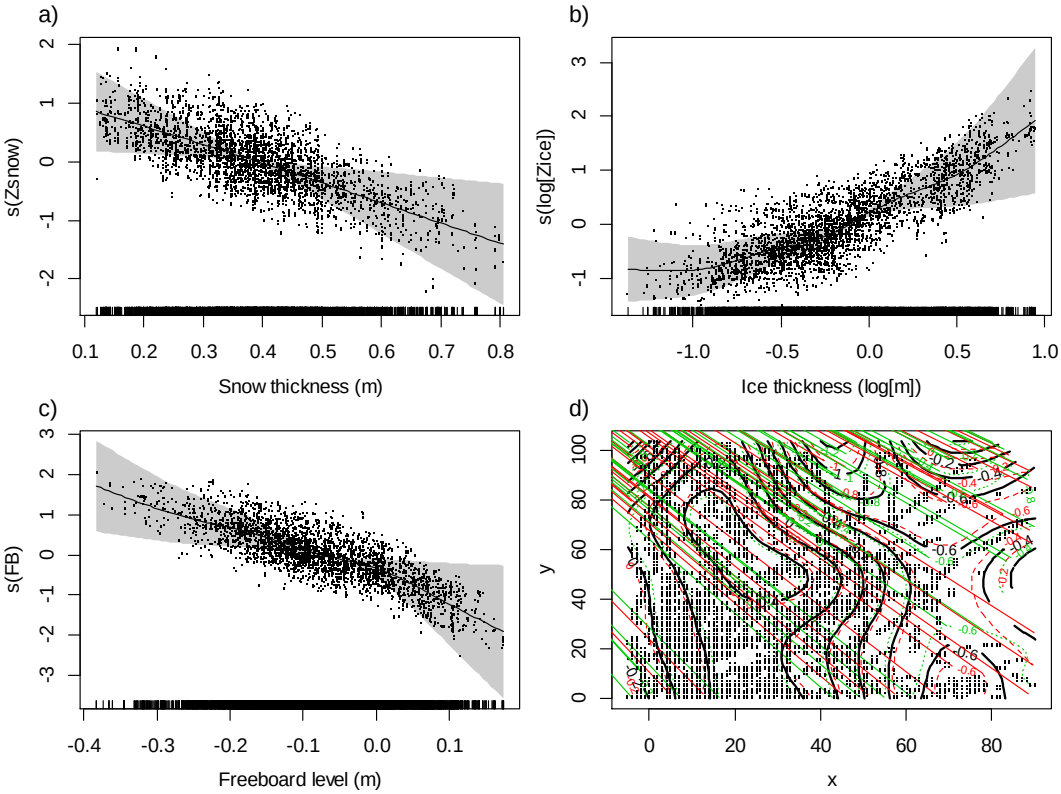

Figure S2: Smooths of generalized additive modelling (GAM_{xy}) terms presented as in Figure 4 but including also d) the smooth interaction on the spatial x-, and y- co-ordinates. In panel d) the black lines indicate the tensor smooth estimate te(x,y), the red and green dashed lines indicate ±1 S.E, and the points indicate the locations of ROV observations (n = 4425). Note natural log scale on x-axis in panel b.

References (used in supplementary material):

Lange, B. A., Katlein C., Nicolaus M., Peeken, I., and H. Flores (2016), Sea ice algae chlorophyll a concentrations derived from under-ice spectral radiation profiling platforms. *J. Geophys. Res*., doi 10.1002/2016JC011991.

Melbourne-Thomas, J., K. M. Meiners, C. J. Mundy, C. Schallenberg, K. L. Tattersall, and G. S. Dieckmann (2015), Algorithms to estimate Antarctic sea ice algal biomass from under-ice irradiance spectra at regional scales, *Mar. Ecol. Prog. Ser., 536*, 107–121.

Melbourne-Thomas, J., K. M. Meiners, C. J. Mundy, C. Schallenberg, K. L. Tattersall, and G. S. Dieckmann (2016), Corrigendum: Algorithms to estimate Antarctic sea ice algal biomass from under-ice irradiance spectra at regional scales, *Mar. Ecol. Prog. Ser.*, *561*, 261.

Mundy, C. J., J. K. Ehn, D. G. Barber, and C. Michel (2007), Influence of snow cover and algae on the spectral dependence of transmitted irradiance through Arctic landfast first-year sea ice, *J. Geophys. Res.*, *112*, C03007, doi:10.1029/2006JC003683.

Williams, G.D. et al. (2013), Beyond point measurements: Sea ice floes characterized in 3-D. *Eos, Transactions AGU,* 94, 69–70.

Williams, G., et al. (2015), Thick and deformed Antarctic sea ice mapped with autonomous underwater vehicles. *Nature Geo.*, *8*, 61–67, doi:10.1038/NGEO2299.

Wood, S.N. (2006), *Generalized Additive Models: An Introduction with R.,* CRC press.